Oxidation of methyl formate and its interaction with nitric oxide

María U. Alzueta *, Verónica Aranda, Fabiola Monge, Ángela Millera, Rafael Bilbao

Aragón Institute of Engineering Research (I3A), Río Ebro Campus, University of Zaragoza, 50018 Zaragoza, Spain

ABSTRACT

An experimental and kinetic modeling study of the oxidation of methyl formate (MF) has been performed. The experiments have been carried out in an isothermal tubular quartz flow reactor, at atmospheric pressure, in the temperature range 300–1100 K. The influence of the temperature, oxygen concentration and the presence of nitric oxide have been analyzed on the oxidation regime of MF and on the formation of the main products (CH_3OH, CO, CO_2 and H_2). A detailed chemical kinetic mechanism for the oxidation of MF has been used for calculations. The results show that the oxidation regime of MF for different stoichiometries is very similar both, in the absence and in the presence of nitric oxide, but some differences are found under oxidizing conditions in the presence of NO. Under these conditions, a mutually sensitized oxidation of MF and NO is seen to occur. In spite of the fact that a minimum of the concentration of NO is observed, no net reduction of NO_x is found.

© 2013 The Combustion Institute. Published by Elsevier Inc. All rights reserved.

1. Introduction

Methyl formate (MF), $HCOOCH_3$, is a major intermediate in the oxidation of dimethoxymethane (DMM) and may be present as a reaction product in the combustion of dimethylether (DME) in the presence of NO_x [1]. Both DMM and DME are promising diesel fuel additives and/or substitutes [2–7]. Furthermore, MF is also involved in the oxidation of other hydrocarbons and it is the simplest methyl ester, belonging to a class of compounds that constitute biodiesel [8]. Since esters are volatile compounds that are used in the manufacture of perfumes, food flavoring and solvents, or can be released from natural sources [9], the presence of MF in the atmosphere is a reality. The atmospheric oxidation of MF has received attention and different models for describing its oxidation under these conditions have been developed. Good and Francisco [10] reported that, in the atmosphere, there are four different main pathways which lead to the destruction of organic molecules: reaction with OH radical, UV photolysis, reaction with O atoms in their excited states (O^1D) and reaction with chlorine atoms. Some of these reaction pathways might also be important under combustion conditions; in particular, the reaction between MF and OH radicals, which has been theoretically and experimentally studied by different authors. The absolute rate constants for the gas phase reaction of OH radicals with MF were determined by Wallington et al. [11] and Le Calvé et al. [12]. Theoretical studies include the ab initio molecular orbital theory work by Good et al. [13], to determine the relative importance of the products of the hydrogen

abstraction reactions: CH_3OCO and CH_2OCHO, of which CH_3OCO is the predominant radical. Moreover, their rate constant measurements were in agreement with the values obtained by other authors [11,12]. Metcalfe et al. [14] investigate the MF decomposition using high-level ab initio calculations, and Chao et al. [15] studied the photodissociation of methyl formate using the resonance-enhanced multiphoton ionization concluding that the major decomposition channel is the one that produces CH_3OH and CO.

While many studies have been reported in the literature about the decomposition of MF in the atmosphere, few studies addressing pyrolysis and oxidation of MF at high temperatures have been reported.

MF decomposition was subject of the studies of Steacie [16] and Jain and Murwaha [17], who carried out static reactor experiments. Their results were examined with the ab initio molecular orbital theory to determine which reaction pathway was more favorable energetically [18]. Francisco [18] suggested a mechanism which included two competitive parallel reactions, leading to the formation of CH_3OH + CO and CH_2O + CH_2O.

Plausible combustion pathways, under conditions where temperatures can reach on the order of 1000 K and there are significant concentrations of CH_3 radicals and H atoms that may contribute to the comsumption of MF, were studied theoretically by Good and Francisco [10] using ab initio molecular orbital calculations. These authors concluded that the rate of reaction of hydrogen atoms with MF is significantly faster than the analogous reactions initiated by methyl radicals. Very recently, Peukert et al. [19] have experimental and theoretically determined the rate constants for hydrogen abstraction and thermal decomposition of methyl formate, and their results are in agreement with the earlier determinations of Metcalfe et al. [14] and Good and Francisco [10].

---

* Corresponding author. Fax: +34 976761879.
  E-mail address: uxue@unizar.es (M.U. Alzueta).

MF has also been the subject of different kinetic modeling studies under combustion conditions. Fisher et al. [20] developed a detailed kinetic model for the oxidation of methyl formate and methyl butanoate. This mechanism was tested against combustion data obtained at low temperature and sub-atmospheric conditions in static reactor [21–24]. Westbrook et al. [25] developed a detailed chemical kinetic mechanism for a group of four small alkyl esters, consisting of methyl formate, methyl acetate, ethyl formate and ethyl acetate, which was validated by comparisons between computed results and measured intermediate species in fuel-rich, low-pressure, premixed laminar flames [26,27]. These two chemical kinetic models [20,25] were also used to interpret the autoignition of MF mixtures with oxygen/argon and oxygen/nitrogen behind reflected shock waves over the temperature range of 1053–1561 K and 2, 4 and 10 atm [28]. Both mechanisms worked fairly well at 10 atm, but exhibited important deviations with experiments made at lower pressures. Dooley et al. [1] recently constructed a chemical kinetic model which was tested against the experimental data obtained in three different systems: a turbulent flow reactor, a shock tube reactor, and a laminar MF/air flame. This mechanism has recently been used to simulate a low-pressure (22–30 torr) laminar flame and equivalence ratios from 1.0 to 1.8 [8], and the shock tube data of the decomposition of MF recently obtained by Ren et al. [29].

In this context, the present work aims to extend the experimental database with flow reactor data on MF oxidation at atmospheric pressure, and interpret the experimental data in terms of a detailed kinetic modeling study based on the MF mechanism subset by Dooley et al. [1]. Additionally, the impact of MF conversion on the formation of soot and on the interaction with NO is analyzed, by means of pyrolysis experiments of MF and by adding a given amount of NO. The main reactions for MF pyrolysis and oxidation are identified and the impact of the main reactions is evaluated. Specifically, in the present work the oxidation process of MF has been investigated under flow conditions, at atmospheric pressure, in the 300–1100 K temperature interval, from pyrolysis to very fuel-lean conditions, both in the absence and in the presence of NO.

2. Experimental

Oxidation experiments of MF, in the absence and in the presence of NO, have been carried out in an installation which consists basically of a gas feeding system, a reaction system and a gas analysis system. The experimental installation used in the present work is described in detail elsewhere (e.g., [30]) and only a brief description is given here.

Gases are supplied from gas cylinders through mass flow controllers. A constant concentration of approximately 700 ppm of MF is introduced in all the experiments. The amount of O_2 used, which depends on the oxygen excess ratio (λ) defined as the inlet oxygen concentration divided by oxygen necessary for complete combustion, has been varied between 0 and 49,000 ppm. A concentration of approximately 500 ppm of NO has been used in the experiments conducted with nitric oxide. Nitrogen is used to balance, resulting in a constant flow rate of 1340 (STP) mL/min. All the experimental mixtures are diluted in nitrogen. Therefore, little heat is released during the reaction and isothermal conditions can be considered.

The reaction zone of the quartz flow reactor has the dimensions of 5.5 mm inside diameter and 560 mm in length. This quartz flow reactor is placed in a three-zone electrically heated oven, ensuring a uniform temperature profile (±10 K) along the reaction zone. An example of temperature profiles inside the reaction zone can be found as Supplementary material.

The gas residence time, t_r, in the isothermal zone is a function of the temperature, $t_r(s) = 195/T(K)$ (700–190 ms). All the experiments

Table 1

Matrix of experimental conditions. The experiments are conducted at constant flow rate of 1340 (STP) mL/min, at atmospheric pressure, in the temperature interval of 300–1100 K. The balance is closed with N_2. The residence time is dependent on the reaction temperature: $t_r(s) = 195/T(K)$.

Exp	MF (ppm)	O_2 (ppm)	NO (ppm)	λ
Set 1	658	0	0	0
Set 2	664	980	0	0.7
Set 3	683	1400	0	1
Set 4	702	49000	0	35
Set 5	695	0	508	0
Set 6	687	980	505	0.7
Set 7	684	1400	512	1
Set 8	672	49000	492	35

are carried out at atmospheric pressure and in the temperature interval of 300–1100 K. Table 1 lists the conditions of the experiments.

The product gases are quenched at the outlet of the reaction zone. Previous to the gas analysis, gases go through a filter and a condenser to assure gas cleaning. The outlet gas composition is measured using a micro gas cromatograph (Agilent 3000), equipped with TCD detectors, which is able to detect MF, hydrocarbons (CH_4, CH_2O, CH_3OH, C_2H_6, C_2H_4 and C_2H_2), CO, CO_2 and H_2. The NO concentration is measured by means of a continuous IR analyzer (URAS 26, AO2000, ABB). A Fourier Transform Infrared (FTIR) spectrometer (Genesis I, Ati Mattson) is used to check the formation of some nitrogen compounds such us NO_2, HCN and NH_3. The uncertainty of the measurements is estimated as ±5%, except for the FTIR spectrometer, which is estimated as ±10%.

The atomic carbon balance was checked in order to evaluate the goodness of the experiments, and resulted to close always between 90% and 99%.

3. Reaction chemical kinetic mechanism

The present experimental results have been analyzed in terms of a detailed gas-phase chemical kinetic model. The full mechanism takes as starting point the model of Glarborg et al. [31] for the interactions between C_1/C_2 hydrocarbons and NO, updated in a number of works [32–40], which we wish to also extend to account for the oxidation of different oxygenated hydrocarbons and their interaction with NO and other compounds of interest. A reaction subset for MF oxidation, taken mainly from the work of Dooley et al. [1], has been added to the above mechanism. Additional details are related below. The reverse rate constants were obtained from the forward rate constants, and the thermodynamic data were taken from the same sources as the different mechanism subsets.

Under the present combustion conditions, the main reaction pathway is the thermal decomposition of MF to give methanol, formaldehyde and methane, with the channel producing methanol representing about a 90% of the MF consumption. The production of methanol and carbon monoxide from MF has been considered earlier in the literature. Francisco [18] calculated the energy barrier for such decomposition as 74.0–77.0 kcal/mol. Other activation energies values for this reaction have been reported in the literature in the range of 48.7–68.3 kcal/mol [14–17,41]. Thus, there is a considerable uncertainty in the activation energy for such reaction. Dooley et al. [1] chose a value of 60.0 kcal/mol considering an analogy to the decomposition reaction of methyl tert-butyl ether (MTBE) to produce isobutene and methanol. We have used for most calculations the estimation by Dooley et al. [1], but since our results are mostly sensitive to this reaction, in particular to the activation energy chosen, the impact of varying the activation energy for such reaction has been addressed and is shown below. For

the decomposition of the CH_3OCO alkyl radical, the determination of Glaude et al. [42] has been taken, which agrees reasonably with the determinations of McCunn et al. [43] and Huynh and Violi [44].

In order to account for the presence of NO, the mechanism has been completed with hydrocarbon-NO interactions [33,37] and mutually sensitizing effects between NO and NO_2 and hydrocarbons [38–40].

Model calculations have been performed using Senkin, the plug flow reactor code that runs in conjunction with the Chemkin-II library [45,46], assuming pressure and temperature constants in the reaction zone, which has been tested to be a fairly good consideration. The full mechanism listing and thermochemistry used can be found as Supplementary material and can be directly obtained from the authors (uxue@unizar.es).

4. Results and discussion

A study of the oxidation of MF at atmospheric pressure in the 300–1100 K temperature interval has been carried out under flow reactor conditions. In addition to temperature, the influence of the stoichiometry and the presence of NO have been also analyzed. The experimental data have been interpreted in terms of a detailed chemical kinetic mechanism for MF oxidation.

4.1. Oxidation of MF in the absence of NO

Figure 1 shows the influence of temperature and stoichiometry on the concentration of MF and the formation of methanol. Figure 2 presents the corresponding results for the concentration of CO, CO_2

and H_2 for the same experimental conditions as Fig. 1. The concentration profiles are shown as function of temperature for different stoichiometries, corresponding to sets 1–4 in Table 1. These figures compare experimental (symbols) and simulation results (lines). The model predicts very well the general trends of the concentration profiles.

The temperature for the onset of the conversion of MF is slightly above 800 K independently of the stoichiometry, with MF completely converted in all the cases at 1100 K approximately, even under pyrolysis conditions. This observation can be attributed to the fact that thermal decomposition of MF appears to be the main conversion pathway. The oxygen concentration in the reactant mixture does not significantly influence the decay of MF, what matches with the oxidation behavior observed for other oxygenated compounds such as dimethylether [34] or dimethoxymethane [47]. However, the oxygen availability is seen to have a slightly more noticeable effect on some of the reaction products. The

Fig. 1. Influence of the stoichiometry on the MF and CH_3OH concentration profiles as a function of temperature in the absence of NO. Comparison between experimental data (symbols) and model predictions (lines). The inlet conditions correspond to sets 1–4 in Table 1.
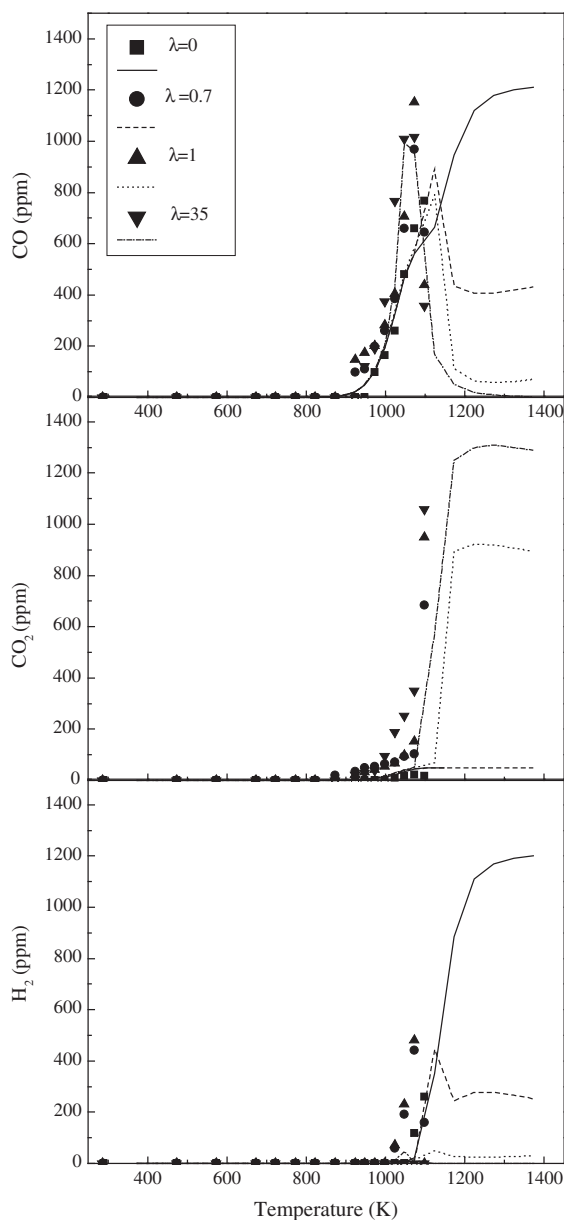
Fig. 2. Influence of the stoichiometry on the CO, CO_2 and H_2 concentration profiles as a function of temperature in the absence of NO. Comparison between experimental data (symbols) and model predictions (lines). The inlet conditions correspond to sets 1–4 in Table 1.

diminution in MF concentration is accompanied by the formation of methanol (Fig. 1), which results to be a main product in all the experiments. Methanol peaks at approximately the same temperature at which the complete conversion of MF is produced. It should be mentioned that neither methane nor formaldehyde have been detected. The formation of CO (Fig. 2) coincides with the decrease in MF, and CO concentration peaks at around 1050 K, which coincides approximately with the maximum of methanol. Once the concentration of CO has reached the maximum concentration, CO_2 exhibits a sharp increase in concentration up to a constant value, as shown in calculations. While for stoichiometric and oxidizing conditions MF is mainly oxidized to CO_2, under reducing conditions a considerable amount of CO is present in the product gas mixture, and under pyrolysis conditions CO_2 is hardly formed. Additionally, we made an additional experiment in a different setup to study the pyrolysis of 2515 ppm MF, in nitrogen as bath gas, at 1500 K and a residence time of 2 s, following the experimental procedure of Esarte et al. [48]. Specifically, in this experiment both concentration and flow rate are significantly higher compared to the rest of experiments of the present work. Because of the higher temperature and dimensions of the reactor and the lower dilution, conditions are more favorable to detect soot formation compared to the high dilution ones of the rest of experiments. However, no formation of soot was found, but 4486 ppm CO, 299 ppm CO_2, 383 ppm CH_4 and 3361 ppm H_2 were obtained. H_2 is detected for all the present conditions, except for oxidizing conditions, at temperatures higher than 1000 K. Also, it is worthwhile to mention that no methanol and other oxygenates were detected in this experiment, which is coherent considering the high temperature, 1500 K, of this pyrolysis experiment. The model predicts fairly well the main experimental trends, even though slight discrepancies are found.

Figure 3 shows a reaction path diagram for MF oxidation in the absence of NO, obtained with the mechanism compiled here and applied to the conditions of the present work. MF oxidation is initiated by the following decomposition reaction,

$$HCOOCH_3(+M) \rightleftharpoons CH_3OH + CO(+M), \tag{1}$$

with minor relevance of:

$$HCOOCH_3(+M) \rightleftharpoons CH_2O + CH_2O(+M), \tag{2}$$

$$HCOOCH_3(+M) \rightleftharpoons CH_4 + CO_2(+M). \tag{3}$$
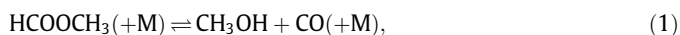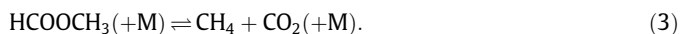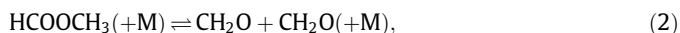
This is in agreement with the results obtained by Dooley et al. [1], who concluded that MF is consumed almost exclusively by elimination reactions, with little importance of hydrogen abstraction reactions.

The methanol produced is consumed by a number of hydrogen abstraction reactions, giving mainly hydroxymethyl radicals,

$$CH_3OH + H \rightleftharpoons CH_2OH + H_2, \tag{4}$$

$$CH_3OH + OH \rightleftharpoons CH_2OH + H_2O, \tag{5}$$

$$CH_3OH + O \rightleftharpoons CH_2OH + OH. \tag{6}$$

Methanol may also form methoxy radicals by hydrogen abstraction reactions with H and OH radicals, even though these channels are much less important under the studied conditions,

$$CH_3OH + H \rightleftharpoons CH_3O + H_2, \tag{7}$$

$$CH_3OH + OH \rightleftharpoons CH_3O + H_2O. \tag{8}$$

The relative importance of all these reactions depends on the availability of oxygen. Both, hydroxymethyl and methoxy radicals either decompose thermally or react with molecular oxygen to give formaldehyde,
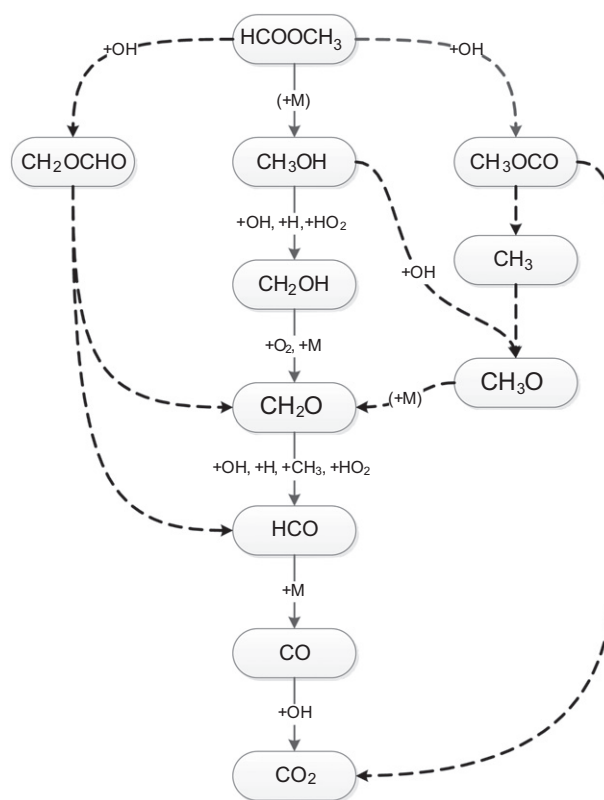
Fig. 3. Reaction path diagram for MF oxidation according to the current kinetic model. The dashed line refers to the additional paths occurring under oxidizing conditions.

$$CH_2OH(+M) \rightleftharpoons CH_2O + H(+M), \tag{9}$$

$$CH_2OH + O_2 \rightleftharpoons CH_2O + HO_2, \tag{10}$$

$$CH_3O(+M) \rightleftharpoons CH_2O + H(+M). \tag{11}$$

Once formaldehyde has been formed, it follows the well known reaction sequence to yield CO_2 as final product: $CH_2O \rightarrow HCO \rightarrow CO \rightarrow CO_2$.

Under oxidizing conditions, MF also decomposes via hydrogen abstraction reactions in order to produce radicals CH_2OCHO and CH_3OCO radicals, i.e.:

$$HCOOCH_3 + OH \rightleftharpoons CH_2OCHO + H_2O, \tag{12}$$

$$HCOOCH_3 + OH \rightleftharpoons CH_3OCO + H_2O. \tag{13}$$
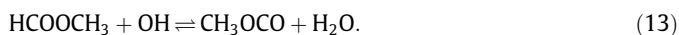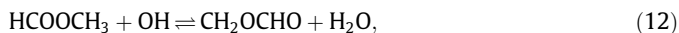
Both radicals decompose thermally, CH_2OCHO to give formaldehyde and formyl radical and CH_3OCO to form methyl radical and CO_2, through reactions 14 and 15 respectively.

$$CH_2OCHO \rightleftharpoons CH_2O + HCO, \tag{14}$$

$$CH_3OCO \rightleftharpoons CH_3 + CO_2. \tag{15}$$

Methanol also forms methoxy radicals by hydrogen abstraction reactions with OH radicals in oxidizing conditions,

$$CH_3OH + OH \rightleftharpoons CH_3O + H_2O, \tag{16}$$

with methoxy radicals giving formaldehyde through reaction 11.

A first-order sensitivity analysis for CO has been performed at the temperature of 950 K of all the sets in Table 1, and the results are shown in Table 2. The data of Table 2 indicate that MF conversion is, in general, sensitive to the same reactions independently

Table 2
Linear sensitivity coefficients for CO at the temperature of 950 K for Sets 1–8. (The sensitivity coefficients are given as $A_i \delta Y_j / Y_j \delta A_i$, where A_i is the pre-exponential constant for reaction i and Y_j is the mass fraction of jth species. Therefore, the sensitivity coefficients listed can be interpreted as the relative change in predicted concentration for the species j caused by increasing the rate constant for reaction i by a factor of 2).

Reaction	Set 1	Set 2	Set 3	Set 4	Set 5	Set 6	Set 7	Set 8
$HCOOCH_3(+M) \rightleftharpoons CH_3OH + CO(+M)$	0.940	0.940	0.940	0.932	0.940	0.940	0.940	0.012
$HCOOCH_3(+M) \rightleftharpoons CH_4 + CO_2(+M)$	−0.003	−0.003	−0.003	−0.003	−0.003	−0.003	−0.003	−0.002
$HCOOCH_3(+M) \rightleftharpoons CH_2O + CH_2O(+M)$	−0.001	−0.001	−0.001	0.000	−0.001	−0.001	−0.001	0.011
$HCOOCH_3 + H \rightleftharpoons CH_2OCHO + H_2$	0.000	0.000	0.000	0.000	0.000	0.000	0.000	−0.010
$HCOOCH_3 + H \rightleftharpoons CH_3OCO + H_2$	0.000	0.000	0.000	0.000	0.000	0.000	0.000	−0.009
$HCOOCH_3 + OH \rightleftharpoons CH_2OCHO + H_2O$	0.000	0.000	0.000	0.000	0.000	0.000	0.000	0.202
$HCOOCH_3 + OH \rightleftharpoons CH_3OCO + H_2O$	0.000	0.000	0.000	0.000	0.000	0.000	0.000	0.003
$HCOOCH_3 + O \rightleftharpoons CH_2OCHO + OH$	0.000	0.000	0.000	0.000	0.000	0.000	0.000	0.027
$HCOOCH_3 + O \rightleftharpoons CH_3OCO + OH$	0.000	0.000	0.000	0.000	0.000	0.000	0.000	−0.007
$HCOOCH_3 + O_2 \rightleftharpoons CH_2OCHO + HO_2$	0.000	0.000	0.000	0.000	0.000	0.000	0.000	0.022
$HCOOCH_3 + CH_3 \rightleftharpoons CH_2OCHO + CH_4$	0.000	0.000	0.000	0.000	0.000	0.000	0.000	0.009
$CH_3OCO \rightleftharpoons CH_2OCHO$	0.000	0.000	0.000	0.000	0.000	0.000	0.000	−0.005
$CH_2O + HCO \rightleftharpoons CH_2OCHO$	0.000	0.000	0.000	0.000	0.000	0.000	0.000	0.036
$O + OH \rightleftharpoons O_2 + H$	0.000	0.000	0.000	0.000	0.000	0.000	0.000	0.173
$H + O_2 + N_2 \rightleftharpoons HO_2 + N_2$	0.000	0.000	0.000	0.000	0.000	0.000	0.000	−0.113
$HCO + M \rightleftharpoons H + CO + M$	0.000	0.000	0.000	0.000	0.000	0.000	0.000	0.205
$HCO + O_2 \rightleftharpoons HO_2 + CO$	0.000	0.000	0.000	0.000	0.000	0.000	0.000	−0.206
$CH_3 + CH_3(+M) \rightleftharpoons C_2H_6(+M)$	0.000	0.000	0.000	0.000	0.000	0.000	0.000	−0.009
$CH_3 + O_2 \rightleftharpoons CH_3O + O$	0.000	0.000	0.000	0.000	0.000	0.000	0.000	0.014
$CH_3 + O_2 \rightleftharpoons CH_2O + OH$	0.000	0.000	0.000	0.000	0.000	0.000	0.000	0.025
$CH_3O_2 + CH_3 \rightleftharpoons CH_3O + CH_3O$	0.000	0.000	0.000	0.000	0.000	0.000	0.000	0.004
$CH_2O + O_2 \rightleftharpoons HCO + HO_2$	0.000	0.000	0.000	0.000	0.000	0.000	0.000	0.013
$NO + O + M \rightleftharpoons NO_2 + M$	0.000	0.000	0.000	0.000	0.000	0.000	0.000	−0.007
$HCO + NO \rightleftharpoons HNO + CO$	0.000	0.000	0.000	0.000	0.000	0.000	0.000	−0.013
$CH_3 + NO \rightleftharpoons HCN + H_2O$	0.000	0.000	0.000	0.000	0.000	0.000	0.000	−0.007
$CH_3 + NO \rightleftharpoons H_2CN + OH$	0.000	0.000	0.000	0.000	0.000	0.000	0.000	0.005
$HCO + NO_2 \rightleftharpoons NO + CO_2 + H$	0.000	0.000	0.000	0.000	0.000	0.000	0.000	0.008
$CH_3 + NO_2 \rightleftharpoons CH_3O + NO$	0.000	0.000	0.000	0.000	0.000	0.000	0.000	0.079
$CH_3OH + NO_2 \rightleftharpoons HONO + CH_2O$	0.000	0.000	0.000	0.000	0.000	0.000	0.000	0.005
$CH_3O + NO \rightleftharpoons HNO + CH_2O$	0.000	0.000	0.000	0.000	0.000	0.000	0.000	−0.005

on the stoichiometry and presence of NO, with the results being mostly sensitive to the unimolecular decomposition of MF to give methanol and carbon monoxide, and in a minor extent to other MF decomposition reactions. Only for the leaner conditions in the presence of NO, the results appear to be sensitive to many different reactions, which is attributed to the increased importance of the radical pool for these conditions. Since there is a considerable uncertainty in the activation energy for the reaction HCO-OCH$_3$(+M) $\rightleftharpoons$ CH$_3$OH + CO(+M), the influence of the potential change of the activation energy value between 50.0 and 68.3 kcal/mol, corresponding to the values found on literature, has been evaluated. As an example, the impact of varying the activation energy for this reaction for a given temperature is shown in Figs. 4 and 5 for experiment 1 in Table 1 (pyrolysis conditions in the absence of NO). It is seen that effectively a significant modification of results with varying the activation energy occurs; specifically related to the temperature for the onset of the MF conversion, which is shifted to lower temperatures as the activation energy decreases. Taking into account the results obtained for all the experiments, the influence of the activation energy has been analyzed. Considering the results for a given temperature (1000 K) the value of the reaction rate, that best fits the results, has been determined for the corresponding reaction and temperature. This value can correspond to different values of E$_a$ and k$_0$, values that have been used for calculating the results for the different temperatures. It has been obtained that the impact of the activation energy value appears to be significant, with the value of 60.0 kcal/mol the best to globally match all the experimental data of the present work. The only exception are the data in the presence of NO and lean conditions, Fig. 9, where, as seen below, the calculations are shifted to higher temperatures compared to experimental data. Thus, studies addressing a precise determination of this activation energy would be of interest.
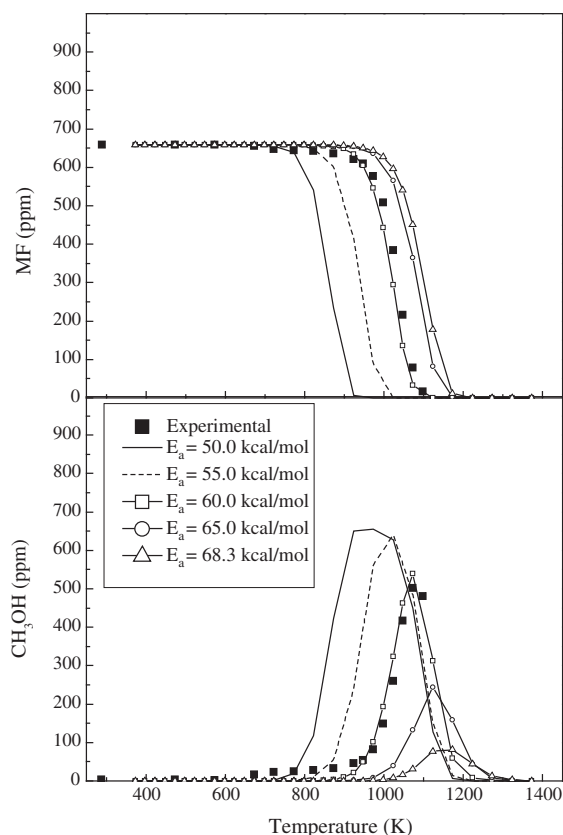
Fig. 4. Influence of the activation energy of the HCOOCH$_3$(+M) $\rightleftharpoons$ CH$_3$OH + CO(+M) reaction on the MF and CH$_3$OH concentration profiles as a function of temperature under pyrolysis conditions. Comparison between experimental data (symbols) and model predictions (lines). The inlet conditions correspond to set 1 in Table 1.
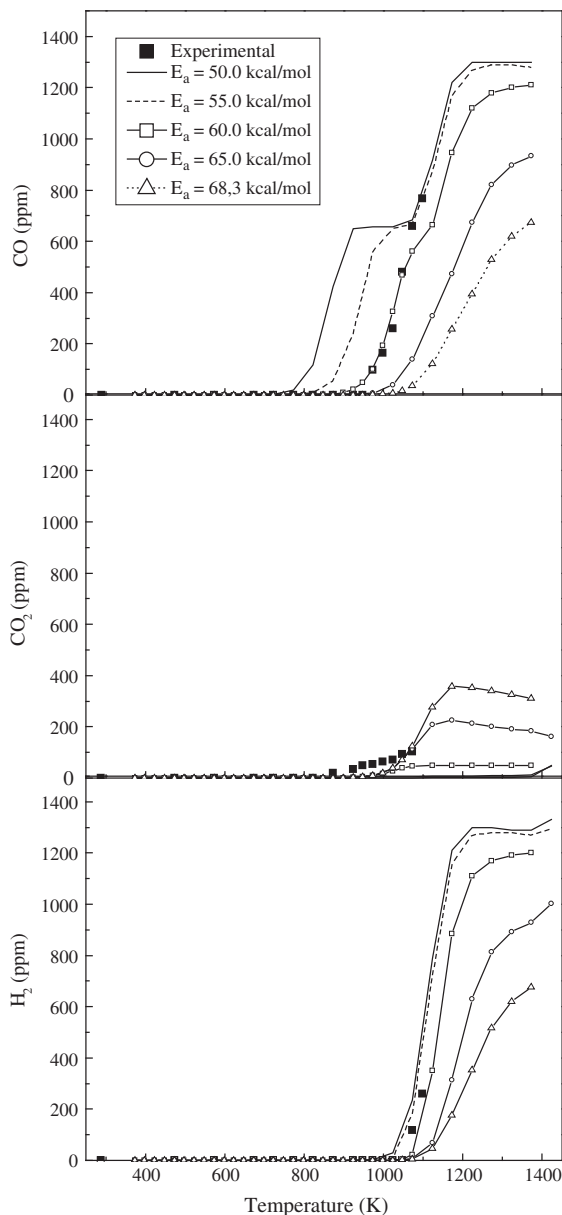
Fig. 5. Influence of the activation energy of the $HCOOCH_3(+M) \rightleftharpoons CH_3OH + CO(+M)$ reaction on the CO, CO_2 and H_2 concentration profiles as a function of temperature under pyrolysis conditions. Comparison between experimental data (symbols) and model predictions (lines). The inlet conditions correspond to set 1 in Table 1.

4.2. Oxidation of MF in the presence of NO

MF can be formed as intermediate in the combustion of DMM and DME, and may also potentially be used as an additive to diesel fuels. For these reasons, and since NO_x can be produced within the combustion chamber of an engine, the study of the influence of NO presence on MF oxidation and NO conversion has been considered for different stoichiometries.

When nitric oxide is present in the reactant mixture no appreciable differences have been found neither for the MF reaction routes nor for the temperature of the MF oxidation regime, except for oxidizing conditions. Therefore, the comparison between the results obtained in the absence and in the presence of NO is only shown in this work for oxidizing conditions in Figs. 6 and 7.

Comparing the results in Fig. 6, it is seen that the presence of NO shifts the decay of MF toward lower temperatures. Under these lean conditions, the presence of NO has a significant effect, and
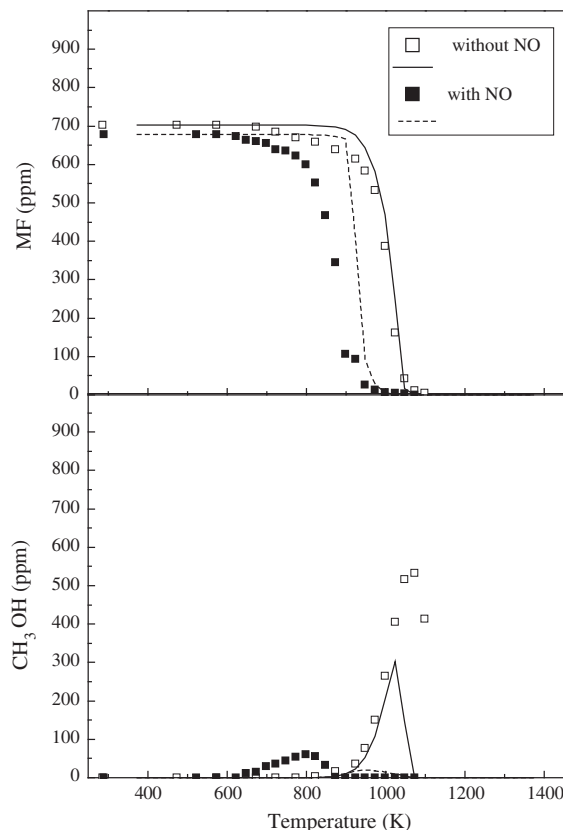
Fig. 6. Influence of the presence of NO on the MF and CH_3OH concentration profiles as a function of temperature under oxidizing conditions. Comparison between experimental data (symbols) and model predictions (lines). The inlet conditions correspond to sets 4 and 8 in Table 1.

the path abstracting hydrogen from MF by action of OH radicals becomes a very active route producing CH_2OCHO radicals, which quickly convert into formaldehyde and formyl radicals, provoking thus the MF conversion at lower temperatures.

Sensitization of MF conversion by action of NO occurs by the conversion of NO to NO_2 under lean conditions, together with the interactions of NO with HO_2, which converts the fairly unreactive HO_2 radical into reactive hydroxyl radicals

$$NO + HO_2 \rightleftharpoons NO_2 + OH, \tag{17}$$

which grow in significant amounts under the lean conditions of Fig. 6, to activate the above mentioned MF + OH reaction path: reaction 17, followed by reactions 12 and 13. This sensitizing effect of conversion of hydrocarbon compounds and NO, happening in the present work between NO and MF, is a well known phenomenon that has been described in a number of works (e.g., [38–40]).

The presence of NO has also an important influence on the methanol profile, with a lower concentration of methanol for the maximum observed. Under these conditions, the presence of NO at fuel lean stoichiometries is responsible for a sensitized oxidation of methanol, which was described in earlier studies of methanol-NO interactions (e.g., [49]). The presence of CO and CO_2 is directly related to the MF concentration profile, Fig. 7. The model is able to reproduce the main trends experimentally observed, even though there are certain discrepancies related to the specific concentration values.

Figure 8 presents the reaction pathways for NO conversion for all the present conditions obtained with the mechanism of the present work. While, as mentioned above, the mutually sensitized oxidation of MF and NO is significant under oxidizing conditions,
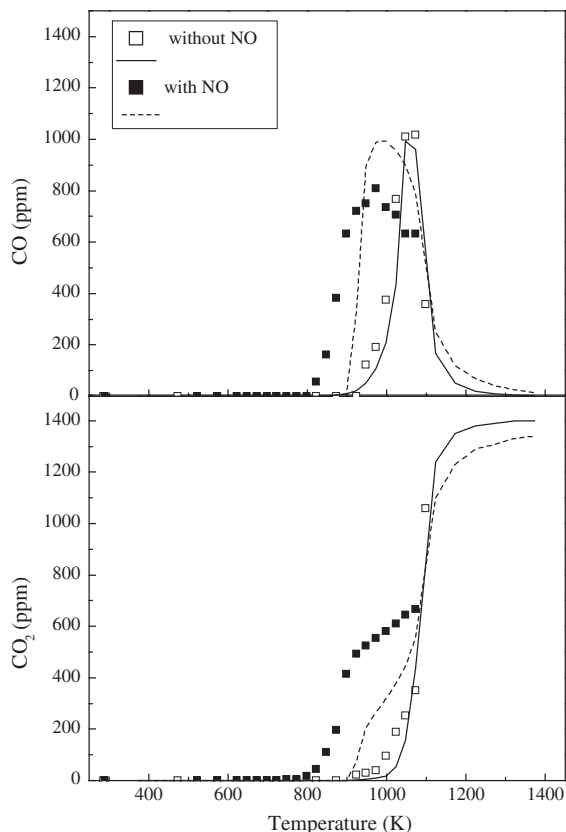
Fig. 7. Influence of the presence of NO on the CO and CO_2 concentration profiles as a function of temperature under oxidizing conditions. Comparison between experimental data (symbols) and model predictions (lines). The inlet conditions correspond to sets 4 and 8 in Table 1.
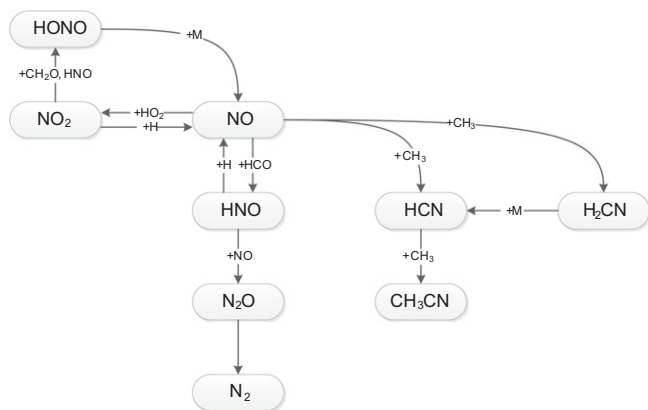
Fig. 8. Reaction path diagram for NO conversion according to the current kinetic model.

also other reaction routes are seen to be important for the other stoichiometries considered.

Under reducing and pyrolysis conditions, calculations indicate that the predominant channel for NO conversion leads also to the formation of HNO through the following route,

$$HCO + NO \rightleftharpoons CO + HNO. \tag{18}$$

And HNO is found to be recycled back to NO by,

$$HNO + H \rightleftharpoons H_2 + NO. \tag{19}$$
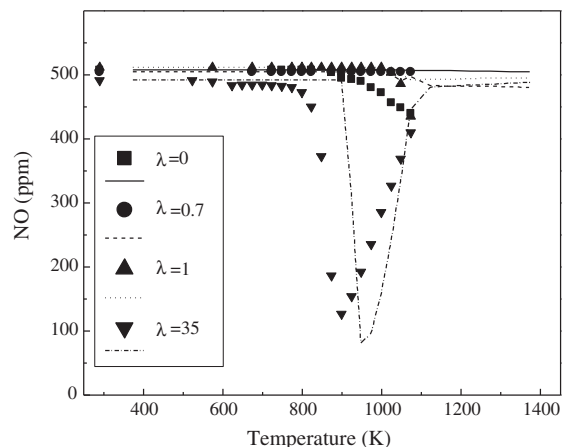
Fig. 9. Influence of the stoichiometry on the concentration profiles of NO as a function of temperature. Comparison between experimental data (symbols) and model predictions (lines). The inlet conditions correspond to sets 5–8 in Table 1.

In these conditions, reburn reactions can also be expected to take place through two different reaction chains: $NO \rightarrow H_2CN \rightarrow HCN$ and $NO \rightarrow HNO \rightarrow N_2O \rightarrow N_2$. So, both channels, the one producing HCN and the one producing N_2O could potentially contribute to NO reduction. However, the present experimental results and calculations indicate that none of these pathways is as relevant as the reaction route mentioned above, i.e. $HCO + NO$ producing HNO which is recycled back to NO. Actually, no HCN and/or N_2O have been detected experimentally in significant amounts in any of the conditions evaluated.

Under reducing and stoichiometric conditions, the NO_2, present because of the NO/NO_2 equilibrium,

$$NO + HO_2 \rightleftharpoons NO_2 + OH, \tag{20}$$

$$NO_2 + H \rightleftharpoons NO + OH, \tag{21}$$

leads to the formation of NO and HONO through the reactions

$$HNO + NO_2 \rightleftharpoons HONO + NO, \tag{22}$$

$$NO_2 + CH_2O \rightleftharpoons HONO + HCO, \tag{23}$$

$$HONO(+M) \rightleftharpoons NO + OH(+M). \tag{24}$$

Finally, Fig. 9 shows the experimental and modeling results for the concentration profiles of NO as a function of temperature for the different stoichiometries. The concentration of NO experiences a noticeable variation only under oxidizing conditions. In this case, NO reaches experimentally a minimum of concentration at approximately 900 K, because of its conversion to NO_2. NO_2 has been quantified in the experiments at the same temperatures as the NO decreases, and the sum of NO and NO_2 at each temperature completes the total amount of NO fed into the system. Thus, no net NO_x reduction occurs. For all the present conditions, NO concentration undergoes a slight decrease at temperatures above 1000 K, even though no other nitrogen species has been detected experimentally. The highest reduction of NO (lower than 10%) is reached at reducing conditions at the highest temperature of the interval studied. However, neither typical reburning species have been detected experimentally, nor they have been predicted by the model.

5. Conclusions

The oxidation of MF has been studied in a tubular quartz flow reactor at atmospheric pressure and in the 300–1100 K tempera-

ture interval, for different stoichiometries, ranging from pyrolysis to oxidizing conditions. The experimental results have been interpreted in terms of a detailed chemical kinetic mechanism.

The experimental results indicate that the stoichiometry does not have a significant influence on the oxidation of MF, while its effect on the main reaction products (CH_3OH, CO, CO_2 and H_2) is more appreciable. In all the present experiments in the absence of NO, the onset of the MF conversion is produced at a temperature slightly above 800 K, being MF completely oxidized at around 1100 K.

The addition of NO does not produce any variation of the MF conversion, except for oxidizing conditions. In this case, the presence of NO results in a mutually sensitized oxidation of the methanol formed from MF and NO, which leads to a sharper decay of methanol and a shift of the end of the conversion to lower temperatures. For all the experiments, the concentration of NO exhibits a slight decrease at the highest temperatures considered, reaching the lowest NO concentration for reducing conditions. Nevertheless, typical reburn species are not detected experimentally or numerically. The result is that the consumption of MF does not result in net decrease of NO_x under the studied conditions, and the sum of the outlet NO and NO_2 concentrations roughly equals the inlet NO concentration.

Both in the absence and presence of NO, the oxidation of MF occurs through a similar reaction pathway, and follows basically the sequence: MF → CH_3OH → CH_2OH/CH_3O → CH_2O → HCO → CO → CO_2. The modeling results have shown that the main reaction channel for MF conversion is its thermal decomposition, independently on stoichiometry, and the results are found to be very sensitive to the activation energy for the $HCOOCH_3(+M) \rightleftharpoons CH_3OH + CO(+M)$ reaction. Modeling results are, in general, able to predict the main trends of the experimental data, even though some discrepancies are found.

Acknowledgments

Appendix A. Supplementary material

Supplementary data associated with this article can be found, in the online version, at http://dx.doi.org/10.1016/j.combustflame.2013.01.005.

References

[1] S. Dooley, M.P. Burke, M. Chaos, Y. Stein, F.L. Dryer, V.P. Zhukov, O. Finch, J.M. Simmie, H.J. Curran, Int. J. Chem. Kinet. 42 (42) (2010) 527–549.
[2] S.C.J. Sorenson, Eng. Gas Turbines Power Trans. ASME 123 (2001) 652–658.
[3] R. Song, K. Li, Y. Feng, S. Liu, Energy Fuels 23 (2009) 5460–5466.
[4] S.H. Yoon, J.P. Cha, C.S. Lee, Fuel Process. Technol. 91 (2010) 1364–1372.
[5] M.B. Sirman, E.C. Owens, K.A. Whitney, SAE Technical Papers no. 2000-01-2048, 2000.
[6] K.H. Song, T.A. Litzinger, Combust. Sci. Technol. 178 (2006) 2249–2280.
[7] A.P. Sathiyagnanam, C.G. Saravanan, Fuel 87 (2008) 2281–2285.
[8] S. Dooley, F.L. Dryer, B. Yang, J. Wang, T.A. Cool, T. Kasper, N. Hansen, Combust. Flame 158 (2011) 732–741.
[9] T.J. Wallington, M.D. Hurley, T. Maurer, I. Barnes, K.H. Becker, G.S. Tyndall, J.J. Orlando, A.S. Pimentel, M. Bilde, J. Phys. Chem. A 105 (2001) 5146–5154.
[10] D.A. Good, J.S. Francisco, J. Phys. Chem. A 106 (2002) 1733–1738.
[11] T.J. Wallington, P. Dagaut, R.H. Liu, M.J. Kurylo, Int. J. Chem. Kinet. 20 (1988) 177–186.
[12] S. Le Calvé, G. Le Bras, A. Mellouki, J. Phys. Chem. A 101 (1997) 9137–9141.
[13] D.A. Good, J. Hanson, J.S. Francisco, Z. Li, G.R. Jeong, J. Phys. Chem. A 103 (1999) 10893–10898.
[14] W.K. Metcalfe, J.M. Simmie, H.J. Curran, J. Phys. Chem. A 114 (2010) 5478–5484.
[15] M.H. Chao, P.Y. Tsai, K.C. Lin, Phys. Chem. Chem. Phys. 13 (2011) 7154–7161.
[16] E.W.R. Steacie, Proc. R. Soc. London, Ser. A 127 (1930) 314–330.
[17] D.V.S. Jain, B.S. Murwaha, Indian J. Chem. 7 (1969) 901–902.
[18] J.S. Francisco, J. Am. Chem. Soc. 125 (2003) 10475–10480.
[19] S.L. Peukert, R. Sivaramakrishnan, M. Su, J.W. Michael, Combust. Flame 159 (2012) 2312–2323.
[20] E.M. Fisher, W.J. Pitz, H.J. Curran, C.K. Westbrook, Proc. Combust. Inst. 28 (2000) 1579–1586.
[21] B.I. Parsons, C.J. Danby, J. Chem. Soc. (1956) 1795–1798.
[22] B.I. Parsons, C. Hinshelwood, J. Chem. Soc. (1956) 1799–1803.
[23] B.I. Parsons, J. Chem. Soc. (1956) 1804–1809.
[24] D.E. Hoare, T.M. Li, A.D. Walsh, Proc. Combust. Inst. 11 (1967) 879–887.
[25] C.K. Westbrook, W.J. Pitz, P.R. Westmoreland, F.L. Dryer, M. Chaos, P. Osswald, K. Kohse-Höinghaus, T.A. Cool, J. Wang, B. Yang, N. Hansen, T. Kasper, Proc. Combust. Inst. 32 (2009) 221–228.
[26] P. Osswald, U. Struckmeier, T. Kasper, K. Kohse-Hoinghaus, J. Wang, T.A. Cool, N. Hansen, P.R. Westmoreland, J. Phys. Chem. A 111 (2007) 4093–4101.
[27] J. Wang, B. Yang, T.A. Cool, N. Hansen, Int. J. Mass Spectrum. 292 (2010) 14–22.
[28] B. Akih-Kumgeh, J.M. Bergthorson, Energy Fuels 24 (2009) 396–403.
[29] W. Ren, K.Y. Lam, S.H. Pyun, A. Farooq, D.F. Davison, R.K. Hanson, Proc. Combust. Inst., 2012. http://dx.doi.org/10.1016/j.proci.2012.05.071.
[30] M. Abián, C. Esarte, A. Millera, R. Bilbao, M.U. Alzueta, Energy Fuels 22 (2008) 3814–3823.
[31] P. Glarborg, M.U. Alzueta, K. Dam-Johansen, J.A. Miller, Combust. Flame 115 (1998) 1–27.
[32] P. Glarborg, M. Østberg, M.U. Alzueta, K. Dam-Johansen, J.A. Miller, Proc. Combust. Inst. 27 (1998) 219–226.
[33] P. Glarborg, M.U. Alzueta, K. Kjærgaard, K. Dam-Johansen, Combust. Flame 132 (2003) 629–638.
[34] M.U. Alzueta, J. Muro, R. Bilbao, P. Glarborg, Isr. J. Chem. 39 (1999) 73–86.
[35] M.U. Alzueta, J.M. Hernández, Energy Fuels 16 (2002) 166–171.
[36] M.U. Alzueta, M. Borruey, A. Callejas, A. Millera, R. Bilbao, Combust. Flame 152 (2008) 377–386.
[37] M.S. Skjøth-Rasmussen, P. Glarborg, M. Østberg, J.T. Johannessen, H. Livbjerg, A.D. Jensen, T.S. Christensen, Combust. Flame 136 (2004) 91–128.
[38] C.L. Rasmussen, A.E. Rasmussen, P. Glarborg, Combust. Flame 154 (2008) 529–545.
[39] P. Dagaut, P. Glarborg, M.U. Alzueta, Prog. Energ. Combust. 34 (2008) 1–46.
[40] G. Dayma, K. Hadj, K.H. Ali, P. Dagaut, Proc. Combust. Inst. 31 (2007) 411–418.
[41] C.P. Davis, The Pyrolysis of Methyl Formate in Shock Waves. Ph. D. Thesis, University of Mississippi, Oxford, MS, 1983.
[42] P.A. Glaude, W.J. Pitz, M.J. Thomson, Proc. Combust. Inst. 30 (2005) 1111–1118.
[43] L.R. McCunn, K.C. Lau, M.J. Krisch, L.J. Butler, J.W. Tsung, J.J. Lin, J. Phys. Chem. A 110 (2006) 1625–1634.
[44] L.K. Huynh, A. Violi, J. Org. Chem. 73 (2008) 94–101.
[45] A.E. Lutz, R.J. Kee, J.A. Miller, Senkin: A Fortran Program for Predicting Homogeneous Gas Phase Chemical Kinetics with Sensitivity Analysis, Sandia National Laboratories, Report SAND87-8248, 1988.
[46] R.J. Kee, F.M. Rupley, J.A. Miller, Chemkin-II: A Fortran Chemical Kinetics Package for the Analysis of Gas-Phase Chemical Kinetics, Sandia National Laboratories, Report SAND87-8215, 1991.
[47] F. Monge, A. Millera, R. Bilbao, M.U. Alzueta, Oxidation of dimethoxymethane in a flow reactor, WIP Poster, in: 34th Symposium (Int.) on Combustion, Varsaw, 2012.
[48] C. Esarte, A. Millera, R. Bilbao, M.U. Alzueta, Ind. Eng. Chem. Res. 49 (2010) 6772–6779.
[49] M.U. Alzueta, R. Bilbao, M. Finestra, Energy Fuels 15 (2001) 724–729.